

# Effects of joint compliance in quadrupedal locomotion

Mehmet Mutlu<sup>\*,\*\*</sup>, Simon Hauser<sup>\*</sup>, Alexandre Bernardino<sup>\*\*</sup>, Auke Ijspeert<sup>\*</sup>

<sup>\*</sup>Biorobotics Laboratory, EPFL Lausanne, Switzerland, [mehmet.mutlu@epfl.ch](mailto:mehmet.mutlu@epfl.ch)

<sup>\*\*</sup>Computer and Robot Vision Laboratory, IST-ISR Lisbon, Portugal

## 1 Introduction

Compliance is one of the most pronounced characteristics in animals. It is present in almost all parts of the musculoskeletal system of a body: muscles, tendons, tissue, skin and even bones all possess a certain level of compliance. The effects of compliance greatly vary on the momentary task or activity. It has the potential to add robustness to stiff/brittle structures, is able to store and release energy and can help to reduce peak forces e.g. when an impact is experienced. In order to profit from such properties, it is important to note that in most cases the compliance needs to be well-tuned to obtain a desired effect.

In locomotion, compliance is suspected to play a key-role in many aspects from safety and gait stabilization to energy efficiency and dynamic gaits (e.g. [1]), given that the compliance suits a specific mode and gait. It is unclear however, which kind of compliance acts on which aspects and how to quantify potential benefits. Our aim in this work is the development of a robotic platform in the shape of a compliant modular quadruped robot that is able to measure a variety of intrinsic and extrinsic variables to get insight into divers locomotion parameters. The platform is relatively low-budget by mainly using off-the-shelf components, highly customizable and fast to reconfigure due to its modular nature. This allows to rapidly perform experiments on different morphologies with variable structural and compliance properties.

## 2 Modular Quadruped Platform

The robot consists of a rectangular shaped main body (length = 39 cm, width = 23.5 cm) with four limbs (length = 23.5 cm) attached at the edges (see Fig. 1). As limbs, parts of the commercially available modular Bioloid-Kit are used. A limb consists of a dymanixel RX-28 servo motor as the hip and a AX-12A as a knee. Both servo motors are extended with a series elastic element, called the “compliant element”, that can be easily interchanged. The servo motors are controlled via USB by an embedded onboard PC (Odroid-XU4) and have integrated encoders that feed back their position. The controller PC connects to the operator PC via wifi and PC and motors are powered externally (tetherless operation is also possible).

**Compliant modular elements:** The modular elements are made out of two clamps with a compliant element fixed in between (Fig. 1 right). There are three types of elements used in this work: rigid elements out of POM rods (poly-

oxymethylene) and two types of compliant elements out of super-elastic Nitinol wire with diameters of  $d = 1.5$  mm (further called “soft”) and 2 mm (further called “hard”) with corresponding flexural stiffnesses 2.3 Nm/rad and 7.3 Nm/rad; torsional stiffnesses 1.75 Nm/rad and 5.54 Nm/rad [2].

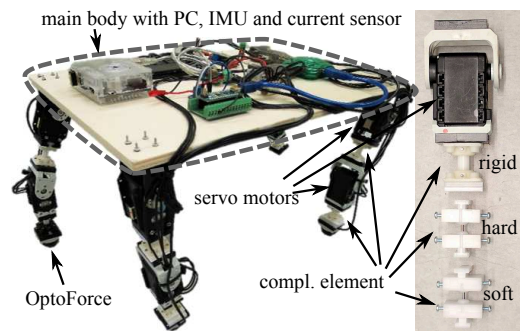


**Figure 1:** Modular quadruped platform. Left: Side view of the robot. It consists of the main body and four limbs, each composed of two servo motors with a compliant element in series. OptoForce sensors are used as feet. Right: one servo motor with the three possible compliant elements.

**Sensors:** The robot possesses the following additional sensors onboard: (i) IMU Xsens MTi-3 AHRS measuring roll, pitch and yaw angles as well as acceleration in x, y and z direction, (ii) analog DC current sensor (INA169) measuring motor power consumption and (iii) 3-axis OptoForce OMD-30-SE-100N force sensors on each foot. Further, the embedded PC is capable of reading the position data from the stream of an external MoCap system and logging all sensor readings with 100 Hz or more (MoCap: 250 Hz, current sensor: 1500 Hz). Thus, all data frames are timestamped with the same clock and they are inherently synchronized.

**Control:** For this preliminary study, a simple open-loop walking trot gait at 0.5 Hz with dutyfactor of 0.5 has been implemented. All the experiments in this study use the same trajectory followed by inverse kinematics by each limb.

## 3 Experiments

The experiments mainly aimed at validating the functionality of the complete system, defining appropriate metrics for the gathered data and performing a limited set of locomotion experiments with changing compliances. Three different types of compliance at eight motors would already result in a large set of experiments if all the combinations would be tested. Since the control is symmetric and the platform laterally quasi-symmetric, only laterally symmetric compliance distributions have been tested. These are:

**Proximal vs. distal joint compliance:** The compliances closer to the main body (proximal) differ from the compliances further from the main body (distal). It was quickly apparent that the robot only locomotes with rigid proximal compliances; hard and soft proximal compliances did not result in any meaningful behavior. Therefore three experiments were performed: rigid, hard and soft distal compliance with rigid proximal compliance.

**Fore vs. hind leg compliance:** Additionally, four experiments to study fore-hind asymmetries were performed. These are hard and soft distal compliances in the fore and hind legs with rigid proximal elements everywhere else.

## 4 Results and Discussions

For each compliance distribution, sensor readings are logged while the robot is walking in steady-state. A concise summary of the results is given in Fig. 2. The most common metrics found in the literature are power consumption, speed and cost of transport (CoT). They are reported as average current (Cur.) drawn by the motors with a constant 18V DC power supply; the distance (Dist.) is taken with the locomotion duration fixed at 20 sec and the ratio of current to distance respectively for the calculation of CoT. The accelerometer (Acc.) and gyro axes show the average euclidean norm of independent x-y-z axes readings. The control error axis is the average position error of the servo motors in all joints while the force fluctuation is the standard deviation of the force sensor readings during the locomotion. Some axes are inverted to position more desired locomotion characteristics further away from the center.

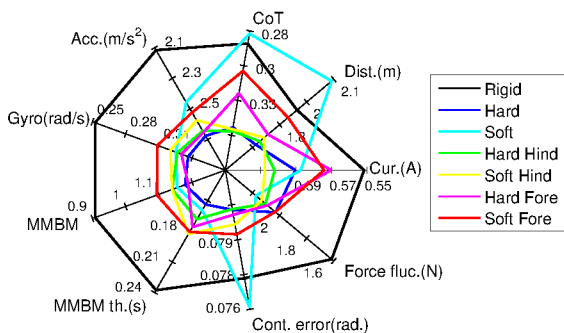


**Figure 2:** Spider plots of all performed compliance distributions where more desired metrics are positioned further away from the center.

**Visual characteristics vs compliance:** The final study is on the correlation between leg compliance and visual characteristics. The metric (MMBM, in short “ $\mu$ ”) given by [3] is used to estimate the motion blur level that occurs on images taken by a fixed onboard camera due to body oscillations. Fig. 3 illustrates the metric value during two gait cycles with different distal compliant element distributions. Furthermore, the average MMBM values during experiments can be seen in Fig. 2. For an MMBM-based image capture method explained in [3], the time spent under a certain threshold (MMBM th.) is as important as the mean  $\mu$ . Hence, it is

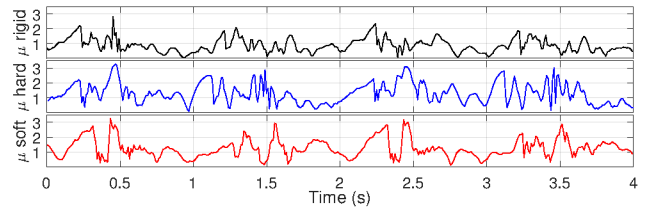


**Figure 3:** MMBM during two gait cycles for three different distal compliance distributions. Higher values correspond to blurrier images if the image is captured at the given time instance by an onboard camera.

also reported in Fig. 2 where the threshold was set to 0.4.

**Limitations of the platform:** The platform has inherent and uncontrolled compliance stemming from the construction materials. Hence, even the rigid case is not completely rigid. Even though it is an animal-like quadruped structure, unlike real animals, the mass is centered more on the legs rather than the body. Moreover, the sticktion of force sensors at feet causes energy accumulation in compliant elements during the locomotion. At takeoff, the compliant leg starts oscillating because of the lack of damping. Such oscillations become significant distortions when the leg mass is relatively high compared the body mass and can be noticed especially in MMBM in the hard case of Fig. 3.

## 5 Conclusion and Future Work

This work reports the design of a modular quadruped platform which enables easy reconfiguration of morphological properties. A variety of sensors record divers locomotion parameters such as position of servo motors, current consumption, acceleration data, ground contact forces, position and orientation which are merged into different metrics. The platform performed its first tests, investigating the effects of joint stiffness distributions. Initial findings indicate that distributions containing hard elements tend to perform worse under the defined metrics whereas a rigid-proximal/soft-distal distribution even outperforms the distinguished all-rigid distribution in certain metrics. Even though the platform does not exactly represent a real animal, we expect to refine our preliminary results, using the full potential of the platform by rapidly performing similar experiments under varying morphological adaptations and locomotion gaits as well as closed loop control using local sensors (as e.g in [4]).

### References

- [1] R. Alexander, “Elastic Energy Stores in Running Vertebrates,” *American Zoologist*, Vol.24, No.1, pp.85–84, 1984.
- [2] M. Vespignani, K. Melo, M. Mutlu and A. J. Ijspeert, “Compliant snake robot locomotion on horizontal pipes,” proceeding in *2015 IEEE International Symposium on Safety, Security, and Rescue Robotics (SSRR)*, West Lafayette, IN, pp. 1-8, 2015.
- [3] M. Mutlu, A. Saranlı and U. Saranlı, “A real-time inertial motion blur metric: Application to frame triggering based motion blur minimization,” proceeding in *2014 IEEE International Conference on Robotics and Automation (ICRA)*, Hong Kong, pp. 671-676, 2014.
- [4] D. Owaki et al., “Simple robot suggests physical interlimb communication is essential for quadruped walking,” *Journal of The Royal Society Interface*, Vol.10, No.78, pp.20120669, 2012.